A tumor suppressor function for caspase-2

Lien Ha Ho[a], Robyn Taylor[a], Loretta Dorstyn[a], Dimitrios Cakouros[a], Philippe Bouillet[b], and Sharad Kumar[a,1]

[a]Centre for Cancer Biology, Hanson Institute, Frome Road, Adelaide, SA 5000, Australia; and [b]The Walter and Eliza Hall Institute of Medical Research, Parkville, Victoria 3050, Australia

Edited by Jerry M. Adams, The Walter and Eliza Hall Institute of Medical Research, Melbourne, Victoria, and approved February 6, 2009 (received for review November 23, 2008)

Apoptosis is mediated by the caspase family of proteases that act as effectors of cell death by cleaving many cellular substrates. Caspase-2 is one of the most evolutionarily conserved caspases, yet its physiological function has remained enigmatic because caspase-2-deficient mice develop normally and are viable. We report here that the *caspase-2*$^{-/-}$ mouse embryonic fibroblasts (MEFs) show increased proliferation. When transformed with E1A and Ras oncogenes, *caspase-2*$^{-/-}$ MEFs grew significantly faster than *caspase-2*$^{+/+}$ MEFs and formed more aggressive and accelerated tumors in nude mice. To assess whether the loss of caspase-2 predisposes animals to tumor development, we used the mouse Eμ-*Myc* lymphoma model. Our findings suggest that loss of even a single allele of *caspase-2* resulted in accelerated tumorigenesis, and this was further enhanced in *caspase-2*$^{-/-}$ mice. The *caspase-2*$^{-/-}$ cells showed resistance to apoptosis induced by chemotherapeutic drugs and DNA damage. Furthermore, *caspase-2*$^{-/-}$ MEFs had a defective apoptotic response to cell-cycle checkpoint regulation and showed abnormal cycling following γ-irradiation. These data show that loss of caspase-2 results in an increased ability of cells to acquire a transformed phenotype and become malignant, indicating that caspase-2 is a tumor suppressor protein.

cell survival | tumorigenesis | cell cycle | proliferation | DNA damage

Evasion of apoptosis is a hallmark of tumorigenesis (1). The cysteine proteases of the caspase family play a key role in the execution of apoptosis (2, 3). In tumor cells many of the defects in apoptosis regulation lie upstream of caspase activation rather than in the caspases themselves (1, 2). Caspase-2 is one of the first discovered and evolutionarily most conserved of caspases (4–6). Although many in vitro studies imply an important role for caspase-2 in DNA damage and stress-induced cell death, *caspase-2*$^{-/-}$ mice are viable and show no overt phenotype (3, 7, 8). This suggests that the role of caspase-2 in cell death is redundant or is compensated by other caspases. However, there is indirect evidence to suggest that caspase-2 may play some role in cancer. For example, the human *caspase-2* gene region on chromosome 7q is frequently affected/deleted in leukemia (9), and caspase-2 and caspase-3 levels have been proposed to be predictors of complete remission and survival in adults with acute lymphoblastic leukemia (ALL) and acute myelogenous leukemia (AML) (10, 11). Furthermore, caspase-2 levels are reduced in mantle cell lymphoma and childhood ALL (12, 13).

Using MEFs from *caspase-2*$^{-/-}$ mice, we recently showed that the loss of caspase-2 results in a delayed apoptosis in response to specific agents (14). We also noted that *caspase-2*$^{-/-}$ MEFs have a higher rate of proliferation than their wild-type counterparts (see below). A link between cell cycle progression and caspase-2 has been identified whereby the cell cycle regulator cyclin D3 was shown to stabilize caspase-2 through possible competition with protease(s) that eliminate the caspase or activate it (15). Furthermore, a recent study suggests that in response to γ-radiation-induced DNA damage, caspase-2 induces apoptosis in a pathway downstream of ataxia telangiectasia mutated (ATM), and ATM and Rad3 related (ATR), following Chk1 inhibition (16). However, it is not known whether the loss of caspase-2 in vivo can potentiate or facilitate tumorigenesis. In the current study we tested this hypothesis using in vitro and in vivo approaches, and we provide evidence that caspase-2 is a tumor suppressor.

Results

Growth Properties of *caspase-2*$^{-/-}$ MEFs. We analyzed the growth properties of *caspase-2*$^{+/+}$ and *caspase-2*$^{-/-}$ MEFs and consistently found that *caspase-2*$^{-/-}$ MEFs had a significantly higher growth rate compared with *caspase-2*$^{+/+}$ MEFs (Fig. 1*A*). Although the data shown in Fig. 1*A* is derived from 3 different batches of cells from 3 animals of each genotype, we have tested at least 8 batches of cells from 8 independent embryos per genotype, all showing similar results (data not shown). To avoid potential selection of cells with higher growth rates, in most of our experiments, MEFs at passages 2–4 were used. We noted that following replating *caspase-2*$^{-/-}$ MEFs appeared to require a somewhat longer recovery period than the matched *caspase-2*$^{+/+}$ MEFs. We then tested whether increased growth rate of *caspase-2*$^{-/-}$ cells leads to their transformation, by analyzing their ability to form colonies in soft agar. We found that both *caspase-2*$^{+/+}$ and *caspase-2*$^{-/-}$ MEFs were unable to do so (Fig. 1*C*).

***Caspase-2*$^{-/-}$ MEFs Transform Readily with E1A and Ras Oncogenes.** Given that *caspase-2* deficiency leads to increased proliferation and some resistance to apoptosis induced by specific agents (Fig. S1), we tested whether the loss of caspase-2 can enhance oncogenic transformation of MEFs. We used a retroviral vector to express E1A and Ras (17) in *caspase-2*$^{+/+}$ and *caspase-2*$^{-/-}$ MEFs and analyzed the properties of cells expressing these oncogenes. The growth rates of E1A/Ras-transformed *caspase-2*$^{-/-}$ MEFs were significantly higher than those of transformed *caspase-2*$^{+/+}$ MEFs (Fig. 1*B*). Furthermore, E1A/Ras-transformed *caspase-2*$^{+/+}$ MEFs formed fewer colonies and at a slower rate compared with the rapid formation of larger colonies by the E1A/Ras-transformed *caspase-2*$^{-/-}$ MEFs in soft agar (Fig. 1 *C* and *D*; data not shown). These findings suggest that the loss of caspase-2 facilitates cell transformation.

E1A/Ras Transformed *caspase-2*$^{-/-}$ Cells Are Highly Tumorigenic in Nude Mice. To evaluate the tumorigenic properties of E1A/Ras-transformed *caspase-2*$^{+/+}$ and *caspase-2*$^{-/-}$ MEFs, we tested their ability to grow in vivo in immunocompromised mice. When injected s.c. in male athymic nude mice, E1A/Ras-transformed *caspase-2*$^{-/-}$ MEFs, from all 8 different batches of MEFs tested, produced rapid and aggressive tumors with all animals developing large tumors within 10 days (all animals injected with E1A/Ras-transformed *caspase-2*$^{-/-}$ MEFs were euthanized before day 15 due to tumor burden; Fig. 2 *A* and *B*). During this period, E1A/Ras-transformed *caspase-2*$^{+/+}$ MEFs from multiple

Author contributions: L.H.H. and S.K. designed research; L.H.H., R.T., L.D., and D.C. performed research; P.B. contributed new reagents/analytic tools; L.H.H., R.T., L.D., D.C., P.B., and S.K. analyzed data; and L.H.H., L.D., and S.K. wrote the paper.

The authors declare no conflict of interest.

This article is a PNAS Direct Submission.

[1]To whom correspondence should be addressed. E-mail: sharad.kumar@imvs.sa.gov.au.

This article contains supporting information online at www.pnas.org/cgi/content/full/0811928106/DCSupplemental.

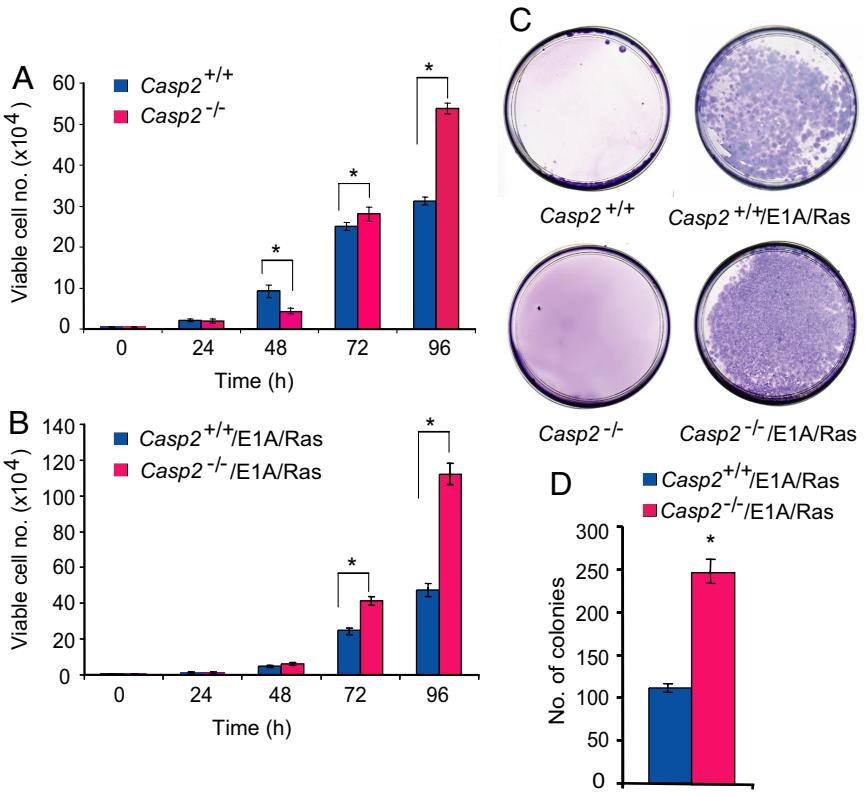

Fig. 1. Growth properties and colony formation by primary and E1A/Ras-transformed *caspase-2*$^{+/+}$ and *caspase-2*$^{-/-}$ MEFs. (*A*) Growth data for *caspase-2*$^{+/+}$ and *caspase-2*$^{-/-}$ MEFs. (*B*) Growth of E1A/Ras-transformed *caspase-2*$^{+/+}$ and *caspase-2*$^{-/-}$ MEFs. (*C* and *D*) Soft-agar colony formation by *caspase-2*$^{+/+}$ and *caspase-2*$^{-/-}$ MEFs and E1A/Ras-transformed *caspase-2*$^{+/+}$ and *caspase-2*$^{-/-}$ MEFs. In panels *A*, *B*, and *D*, results are shown as mean ± SEM from 3 independent experiments using MEFs isolated from 3 different embryos per genotype, and performed in triplicate. *$P < 0.05$.

batches produced small or nondetectable tumors (Fig. 2 *A* and *B*). The average tumor size for caspase-2$^{-/-}$ MEFs at day 10 was ≈3× the average tumor size for *caspase-2*$^{+/+}$ MEFs at day 15 (Fig. 2*B*). Although *caspase-2*$^{+/+}$ and *caspase-2*$^{-/-}$ MEFs were similarly transformed by the E1A/Ras retroviral vector, the delay in the tumor formation and size of tumors produced by transformed *caspase-2*$^{+/+}$ MEFs compared with transformed *caspase-2*$^{-/-}$ MEFs suggest that expression of caspase-2 is required for the inhibition of tumorigenesis.

Caspase-2$^{-/-}$ and E1A/Ras-transformed *caspase-2*$^{-/-}$ MEFs showed significantly reduced sensitivity to apoptosis induced by various cytotoxic drugs and γ-radiation when compared to *caspase-2*$^{+/+}$ and E1A/Ras-transformed *caspase-2*$^{+/+}$ MEFs, respectively (Fig. S1). Re-expression of caspase-2 in primary and E1A/Ras-transformed *caspase-2*$^{-/-}$ MEFs resulted in increased levels of γ-irradiation-induced apoptosis (Fig. S2), suggesting that the levels of caspase-2 probably determine the sensitivity to apoptosis in *caspase-2*$^{-/-}$ MEFs.

As loss of p53 function may also contribute to reduced apoptosis and increased growth rates in *caspase-2*$^{-/-}$ MEFs, we analyzed mRNA expression of cyclin-dependent kinase inhibitor *p21*, a direct transcriptional target of p53 (18), in MEFs at various passages. As expected, *p21* levels were increased in late-passage wild-type MEFs (Fig. S3). Interestingly, no such increase in *p21* transcript was evident in *caspase-2*$^{-/-}$ cells, suggesting that these cells have aberrant p53 function. We did not observe any differences in p53 levels between the wild-type and *caspase-2*$^{-/-}$ MEFs (data not shown). It is thus possible that in late-passage MEFs lacking caspase-2, the function, not the expression, of p53 is abrogated, perhaps by mutations or protein modification.

Lack of caspase-2 Leads to Rapid Onset of Lymphoma in Eμ-*Myc* Mice. To further test whether loss of caspase-2 results in increased susceptibility to tumor formation in vivo, we used the Eμ-*Myc* mouse model (19, 20). As expected, Eμ-*Myc* transgenic mice developed spontaneous lymphomas with a mean onset of illness at 16 weeks. When we combined *caspase-2* deficiency with the Eμ-*Myc* transgene, we saw an accelerated occurrence of tumors compared with Eμ-*Myc* transgenic mice alone (Fig. 3). Interestingly, the loss of a single *caspase-2* allele was sufficient to accelerate tumor formation. The median lifespan of 12 *caspase-2*$^{+/-}$ Eμ-*Myc* mice was 12 weeks with over 90% of mice becoming terminally ill before 50% of *caspase-2*$^{+/+}$ Eμ-*Myc* mice were affected (Fig. 3*A*). Caspase-2$^{-/-}$ Eμ-*Myc* mice had a median lifespan of 8 weeks and became terminally ill within 4 weeks (Fig. 3*B*). Histological examination showed lymphocytic infiltrates in organs, including lung, liver, and lymph nodes (Fig. S4). As in Eμ-*Myc* and *caspase-2*$^{+/-}$ Eμ-*Myc* mice, the tumors induced by *Myc* in *caspase-2*-deficient mice were either B-cell lymphomas or pre-B lymphomas (Table 1).

Loss of the BH3-only protein Bim results in early onset of tumorigenesis in Eμ-*Myc* mice (21). Thus we used *Bim*$^{+/-}$ and *Bim*$^{-/-}$ Eμ-*Myc* mice as controls in our study. *Bim*$^{+/-}$ Eμ-*Myc* mice had a median lifespan of 13 weeks (Fig. 3*A*). The *Bim*$^{-/-}$ Eμ-*Myc* mice median lifespan of 11 weeks was slightly longer than *caspase-2*$^{-/-}$ Eμ-*Myc* mice (Fig. 3*B*). Analysis of peripheral blood showed that there were significantly higher numbers of lymphocytes, particularly the immature lymphoblasts in *Bim*$^{-/-}$ Eμ-*Myc* compared with that of *caspase-2*$^{-/-}$ Eμ-*Myc* and Eμ-*Myc* mice (Fig. 3 *C* and *D*). This indicated that *Bim*$^{-/-}$ Eμ-*Myc* mice had increased leukemia, as expected from previous studies (21), compared with *caspase-2*$^{-/-}$ Eμ-*Myc* or Eμ-*Myc* mice. These observations indicate that, similar to Bim studies, the loss of caspase-2 accelerates morbidity in Eμ-*Myc* mice.

Primary lymphoma cells from *caspase-2*$^{-/-}$ Eμ-*Myc* mice were assessed for their susceptibility to apoptosis induced by various agents. As previously reported for Eμ-*Myc* lymphoma cells (22), *caspase-2*$^{-/-}$ Eμ-*Myc* tumor cells showed high spontaneous apoptosis in culture. Despite high levels of cell death, *caspase-2*$^{+/-}$ and *caspase-2*$^{-/-}$ lymphoma cells showed reduced rates of apoptosis induced by cytotoxic agents when compared with lymphoma cells from Eμ-*Myc* mice (Fig. S5). These findings

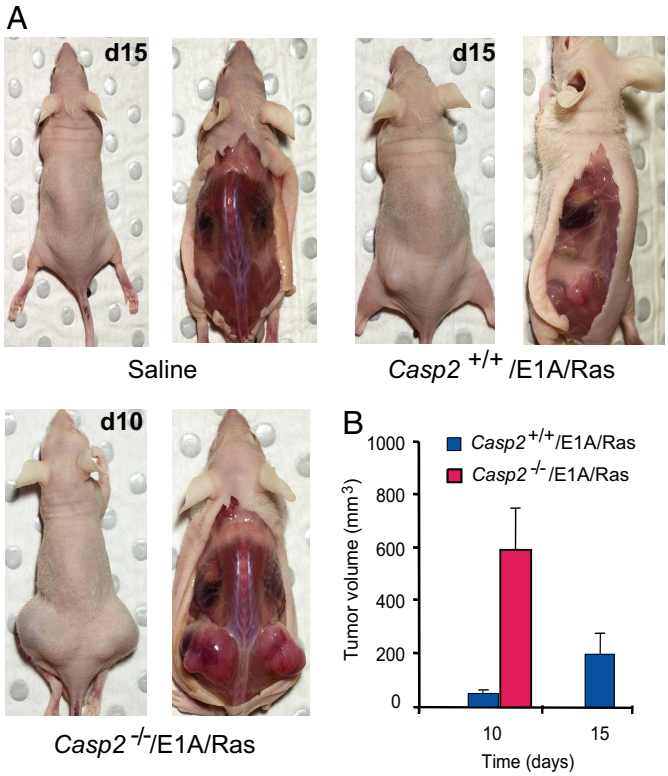

Fig. 2. The lack of caspase-2 accelerates tumor formation in male athymic nude mice. (*A*) Representative mice s.c. injected with saline (LHS panels showing mice at day 15), 1×10^6 E1A/Ras-transformed *caspase-2*$^{+/+}$ (RHS panels showing mice at day 15), or 1×10^6 E1A/Ras-transformed *caspase-2*$^{-/-}$ MEFs (lower RHS panels showing mice at day 10) in the hind flanks. (*B*) Tumor volumes were calculated as described in *Materials and Methods*. The data represent the average tumor volume for the E1A/Ras-transformed *caspase-2*$^{+/+}$ MEFs injected mice ($n = 10$) and E1A/Ras-transformed *caspase-2*$^{-/-}$ (8 different batches) injected mice ($n = 8$) and expressed as mean ± SEM. MEFs derived from 4 animals for each genotype were transformed with E1A/Ras and injected in nude mice. Thus, 2–3 mice received cells derived from a single *caspase-2*$^{+/+}$ or *caspase-2*$^{-/-}$ animal. $P = 1.9 \times 10^{-4}$. Note that all mice injected with E1A/Ras-transformed *caspase-2*$^{-/-}$ MEFs developed large tumors by day 10 and were euthanized before day 15 (thus no data are available for this group at day 15).

Table 1. Frequency of pre-B and B cell tumors induced by the Eμ-*Myc* transgene

Genotype	Pre-B-cell lymphoma frequency	B-cell lymphoma frequency
Eμ-Myc	11 of 21 (52%)	10 of 21 (48%)
Caspase-2$^{+/-}$	6 of 20 (30%)	14 of 20 (70%)
Caspase-2$^{-/-}$	7 of 21 (33%)	14 of 21 (67%)
Bim$^{+/-}$	8 of 20 (40%)	12 of 20 (60%)
Bim$^{-/-}$	9 of 24 (37%)	15 of 24 (63%)

Lymphomas were typed by flow cytometry of surface immunofluorescence; pre-B-cell lymphoma (B220$^+$, CD19$^+$, IgM$^-$) and B-cell lymphoma (B220$^-$, CD19$^-$, IgM$^+$) and expressed as percent pre-B or B lymphoma from total number of lymphomas collected from of each genotype. The frequency of B lymphoma in Eμ-*Myc*, *Bim*$^{+/-}$Eμ-*Myc*, or *Bim*$^{-/-}$Eμ-*Myc* vs. *Caspase-2*$^{+/-}$Eμ-*Myc* or *Caspase-2*$^{-/-}$Eμ-*Myc* mice was not significant.

suggest that caspase-2 contributes to the apoptosis of tumor cells in response to cytotoxic stimuli.

Loss of the DNA Damage Induced Checkpoint Control in *caspase-2*$^{-/-}$ Cells. Caspase-2 is suggested to be involved in p53-dependent apoptosis (3, 8, 23), which could partly explain its tumor suppressor function. However, the growth properties of *caspase-2*-deficient MEFs suggest that it also contributes to cell cycle control. Recent studies using zebrafish and siRNA-mediated knockdown in cell lines suggest that caspase-2 is required in the checkpoint kinase 1 (Chk1)-suppressed apoptotic pathway in p53-deficient cells (16). To test the potential role of caspase-2 in Chk1 pathway, we used *caspase-2*$^{+/+}$ and *caspase-2*$^{-/-}$ MEFs, and E1A/Ras-transformed *caspase-2*$^{+/+}$ and *caspase-2*$^{-/-}$ MEFs. In experiments similar to Sidi et al. (16), we treated cells with the Chk1 inhibitor Gö6976 (which is also known to inhibit PKC) and γ-irradiation. We found that *caspase-2*$^{-/-}$ MEFs were significantly more resistant to apoptosis than the *caspase-2*$^{+/+}$ MEFs treated by either agent alone, as assessed by Annexin V staining and caspase activity measurements (Fig. 4 *A*−*D* and Fig. S6). Interestingly, a reduced sensitivity to apoptosis was observed in *caspase-2*$^{-/-}$ and E1A/Ras-transformed *caspase-2*$^{-/-}$ MEFs when treated with Gö6976 and γ-irradiation together (Fig. 4). These data suggest that caspase-2 has an important role in apoptosis induced by both Chk1-dependent and -inde-

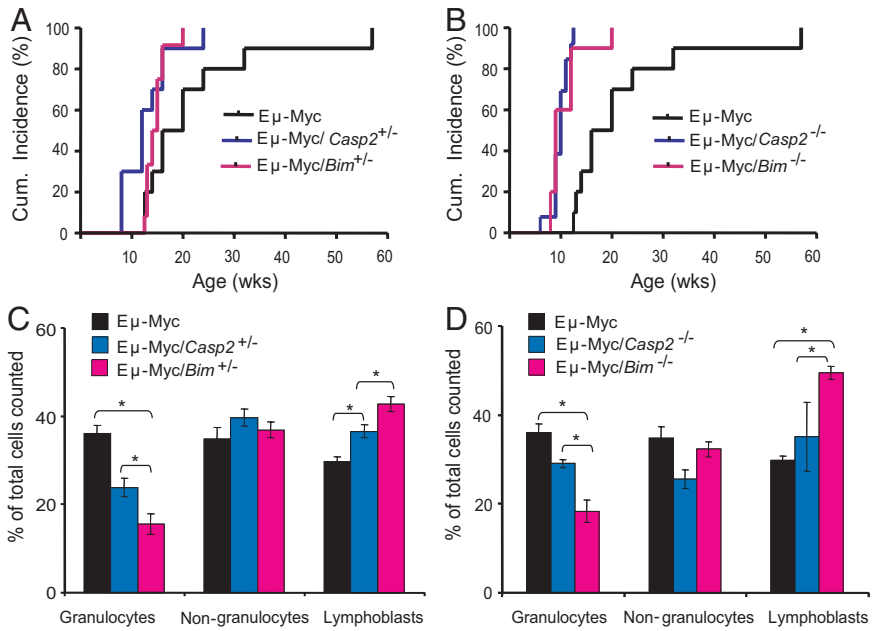

Fig. 3. The loss of caspase-2 accelerates lymphoma development induced by Eμ-*Myc* transgene. (*A*) Cumulative incidence of all tumors in mice of the indicated genotype. Lymphoma development was accelerated in Eμ-*Myc* mice by the loss of one allele of *caspase-2* or *Bim* ($P < 0.001$). (*B*) Lymphoma development was further accelerated in Eμ-*Myc* mice by the loss of both alleles of *caspase-2* or *Bim* ($P < 0.001$). (*C*) Peripheral blood white-cell counts from mice with lymphoma following sacrifice, expressed as percent mean ± SEM of nongranulocytes, granulocytes, and lymphoblasts from total number of cells counted in Eμ-*Myc*, *caspase-2*$^{+/-}$, and *Bim*$^{+/-}$/Eμ-*Myc* mice. (*D*) Peripheral blood white-cell count from mice with lymphoma following sacrifice in Eμ-*Myc*, *caspase-2*$^{-/-}$, and *Bim*$^{-/-}$/Eμ-*Myc* mice. In panels *C* and *D*, cells were counted from blood smears (*$P < 0.001$).

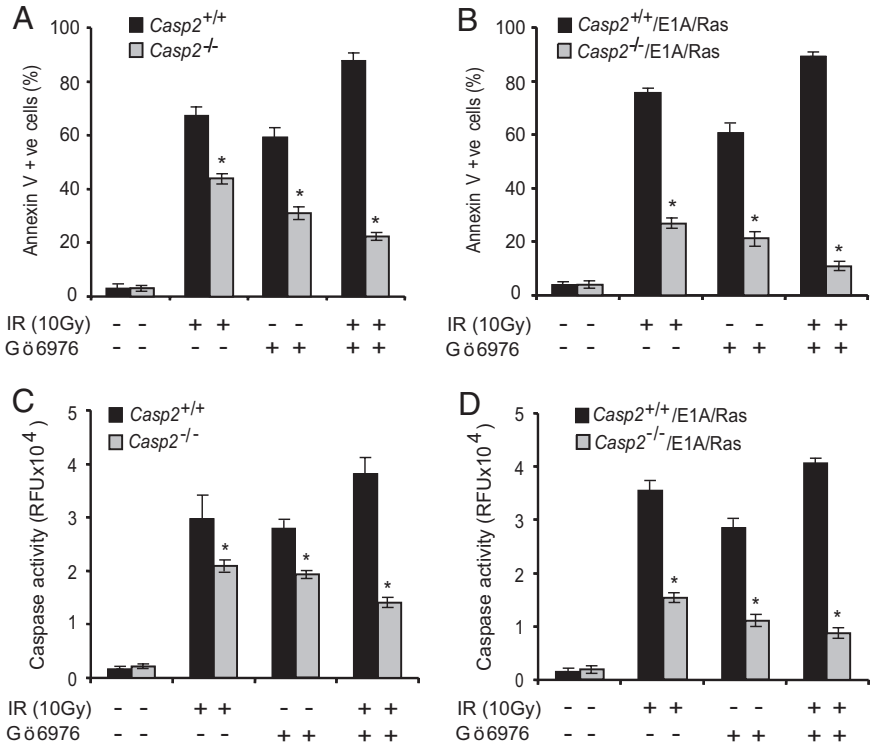

Fig. 4. Caspase-2 contributes to IR-induced apoptosis following Chk1 inhibition. (*A*) Levels of apoptosis in *caspase-2*$^{+/+}$ and *caspase-2*$^{-/-}$ MEFs treated with γ-radiation (10 Gy) and/or Chk1 inhibitor (Gö6976) for 48 h were assessed by Annexin V staining. (*B*) Levels of apoptosis in E1A/Ras-transformed *caspase-2*$^{+/+}$ *and caspase-2*$^{-/-}$ MEFs treated as in panel *A*. Results in panels *A* and *B* are shown as mean ± SEM from 3–4 independent experiments with different batches of MEFs (*$P < 0.05$). Caspase activity in *caspase-2*$^{+/+}$ and *caspase-2*$^{-/-}$, and E1A/Ras-transformed *caspase-2*$^{+/+}$ and *caspase-2*$^{-/-}$ MEFs, was assessed by cleavage of DEVD-AMC (*C* and *D*). Results are expressed as mean ± SEM relative fluorescence units (RFU) from 3 experiments using different batches of MEFs (*$P < 0.05$).

pendent pathways, and when Chk1 is inhibited, apoptosis induced by double-strand DNA breaks becomes even more dependent on caspase-2. It is important to note that in both the *caspase-2*$^{+/+}$ and *caspase-2*$^{-/-}$ cells, caspase activity determined using the substrates VDVAD-AMC and DEVD-AMC was proportional to the number of apoptotic cells. This observation suggests that VDVAD is not a specific substrate of caspase-2 (Fig. 4 *C* and *D* and Fig. S6).

We also tested whether caspase-2 deficiency results in an abnormal response to double-strand DNA breaks. We found that following γ-irradiation a significantly larger proportion of *caspase-2*$^{-/-}$ and E1A/Ras-transformed *caspase-2*$^{-/-}$ MEFs were cycling, as assessed by BrdU staining, compared with *caspase-2*$^{+/+}$ cells (Fig. 5). Cell cycle analysis also indicated that *caspase-2*$^{-/-}$ cells fail to arrest properly following γ-irradiation (data not shown). These findings suggest that caspase-2 deficiency results in abnormal checkpoint regulation following DNA damage.

Discussion

Despite being one of the first caspases to be discovered, the physiological function of caspase-2 has remained enigmatic and controversial. Our studies described here provide strong evidence that caspase-2 is a tumor suppressor. We have shown that the loss of caspase-2 enhances oncogenic potential both in vitro and in vivo. The only other caspase that may have some role in preventing cell transformation is caspase-8. A recent study suggests that following continuous growth in culture, SV40 T antigen immortalized *caspase-8*$^{-/-}$ MEFs become transformed more readily and show increased tumorigenic potential in nude mice than *caspase-8*$^{+/+}$ cells (24). Though these findings suggest that the loss of caspase-8 may contribute to the rate of cell transformation, they are very different from those described here with caspase-2. Primary MEFs from *caspase-2*$^{-/-}$ mice show higher rates of proliferation and are transformed more readily by E1A/Ras than the *caspase-2*$^{+/+}$ MEFs. This suggests that the loss of caspase-2 leads to some deregulation of the cell cycle in vitro, even before oncogenic transformation. Interestingly, we found that *caspase-2*$^{-/-}$ MEFs contain reduced levels of *p21* transcript, when compared with passage-matched wild-type MEFs. As reduced levels of *p21* mRNA expression are indicative of reduced p53 function, we suggest that *caspase-2*$^{-/-}$ MEFs in culture have a tendency to lose p53 function. This may contribute to aberrant growth and apoptotic response observed in *caspase-2*$^{-/-}$ MEFs. Reduced p53 function in *caspase-2*$^{-/-}$ MEFs may also facilitate their transformation by E1A/Ras. That lack of caspase-2 promotes cell transformation was further validated by accelerated onset of tumors seen in athymic nude mice injected with E1A/Ras-transformed *caspase-2*$^{-/-}$ MEFs.

In vivo, accelerated onset of lymphomas was observed in *caspase-2*$^{+/-}$ Eμ-Myc and *caspase-2*$^{-/-}$ Eμ-Myc mice compared with *caspase-2*$^{+/+}$ Eμ-Myc mice, suggesting that even the loss of one allele of *caspase-2* results in accelerated Myc-induced lymphomagenesis. As shown previously (21) and in the control study here, loss of a single allele of *Bim* is also sufficient for increased lymphomagenesis in Eμ-Myc mice. The accelerated Myc-induced lymphomagenesis in *Bim*$^{+/-}$ Eμ-Myc and *Bim*$^{-/-}$ Eμ-Myc mice is consistent with Bim's key role as a regulator of lymphoid and myeloid homeostasis (25–27). However, how the loss of caspase-2 leads to accelerated lymphomagenesis in Eμ-Myc mice remains to be explored. Nevertheless, as caspase-2 levels have been proposed as a predictor of remission and survival in various forms of adult leukemia and its levels are also reduced in certain other cancers (10–13), the observations reported here support an important role for caspase-2 in tumor suppression.

Our data showed that loss of caspase-2 resulted in resistance/delay in apoptosis induced by DNA damage. In γ-irradiated cells, this resistance was further enhanced by the inhibition of Chk1. This observation supports the recent findings suggesting that caspase-2 is involved in an apoptotic pathway downstream of ATM and ATR following Chk1 inhibition (16). Using the same Chk1 inhibitor (which is also known to inhibit PKC), our data showed a significant resistance to apoptosis in irradiated *caspase-2*$^{-/-}$ and E1A/Ras-transformed *caspase-2*$^{-/-}$ MEFs. These results suggest that following DNA double-strand breaks, caspase-2 is required for apoptosis downstream of ATM/ATR

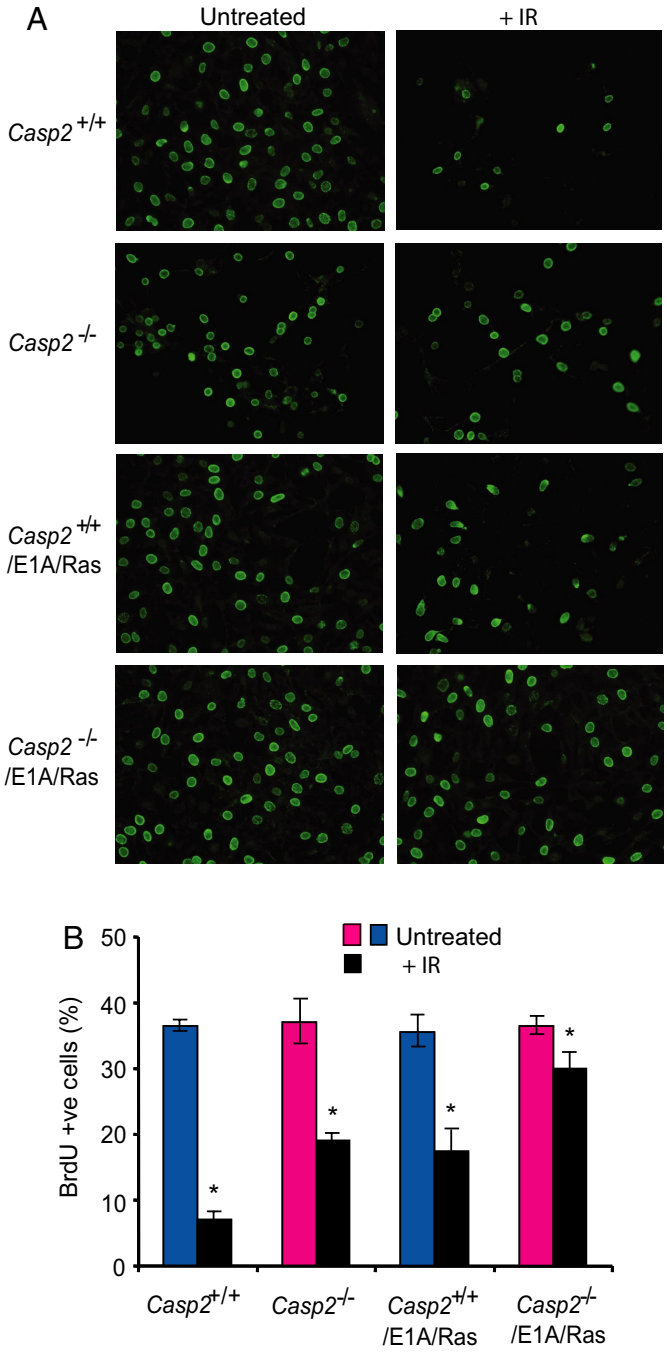

Fig. 5. Caspase-2 contributes to IR-induced cell cycle arrest. (*A* and *B*) Cells stained positive for BrdU 24 h following γ-irradiation. *Caspase-2*$^{+/+}$ or *caspase-2*$^{-/-}$ MEFs, and E1A/Ras-transformed *caspase-2*$^{+/+}$and *caspase-2*$^{-/-}$ MEFs, were seeded onto glass coverslips and exposed to 10 Gy γ-irradiation. Twenty-four hours following γ-irradiation, cells were pulsed for 4 h with BrdU and BrdU +ve cells detected by immunostaining (*A*). Results in panel *B* are expressed as mean ± SEM from 3 experiments. *$P < 0.005$ for comparison between irradiated *caspase-2*$^{+/+}$ vs. *caspase-2*$^{-/-}$ MEFs and E1A/Ras-transformed *caspase-2*$^{+/+}$and *caspase-2*$^{-/-}$ MEFs.

when Chk1 is suppressed. The study by Sidi et al. (16) also suggested that the Chk1-suppressed caspase-2-dependent pathway acts independently of the mitochondrial pathway of apoptosis. In response to stress signaling, caspase-2 has been shown to be activated upstream of mitochondria, and consistent with its initiator function, its activation can occur without processing (28–31). The relative importance of caspase-2 in both apparently distinct apoptotic pathways, and whether there is cross-talk between the pathways, remain to be established.

Unlike other caspases, caspase-2 has a unique ability to localize to the nucleus (30, 32, 33). The predicted cell cycle function of caspase-2 is consistent with its nuclear localization. In preliminary experiments we have noticed that compared with their wild-type counterparts, the late-passage *caspase-2*$^{-/-}$ MEFs and E1A/Ras-transformed *caspase-2*$^{-/-}$ MEFs have an increased tendency to acquire chromosomal aberrations and become aneuploid. This observation suggests that the lack of caspase-2 promotes genetic instability, presumably due to deregulation of cell cycle checkpoints. Although not validated in this study, the increased genetic instability of *caspase-2*$^{-/-}$ MEFs in culture may explain the loss of p53 function in late-passage MEFs. Tumorigenesis is often a consequence of defective apoptosis and cell cycle control. Our data show that the loss of caspase-2 results both in resistance to apoptosis and loss of DNA damage-induced cell cycle regulation, suggesting that caspase-2 is a tumor suppressor. The tumor suppressor role of caspase-2 might explain its reduced expression or loss in many cancers (10–13). Caspases are generally regarded as the downstream effectors of apoptosis, and caspase activation as the point of no return in apoptotic signaling. As such, the role of caspase-2 as a tumor suppressor appears to be unique among mammalian caspases.

Materials and Methods

Proliferation of *caspase-2*$^{+/+}$ and *caspase-2*$^{-/-}$ MEFs. Primary MEFs were derived from wild-type and *caspase-2*$^{-/-}$ embryos at day 13.5 as described (14, 34). MEFs were grown and maintained in high-glucose DMEM and routinely passaged just before reaching confluence. Proliferation of *caspase-2*$^{-/-}$ MEFs was assayed by doubling time experiments and also proliferation assays using CellTiter 96 AQueous One kit (Promega) (data not shown). Similar results were obtained with both assays. For the doubling time experiment, 1×10^4 cells were seeded, and viable cells counted at various time points up to 72 h with trypan blue. Colony-forming assay was performed by resuspending cells (1×10^4) in 0.3% agar in DMEM + 10% FCS and overlaid on 0.6% agar in the same medium in 35-mm culture dishes. The dishes were incubated at 37 °C in 5% CO_2 for 14 days. Colonies were stained in 0.1% toluidine blue in 1% formaldehyde and counted.

Transformation of MEFs. *Caspase-2*$^{+/+}$ and *caspase-2*$^{-/-}$ MEFs were transfected with pWZL-H retroviral vector containing the E1A/Ras oncogenes (obtained from Scott Lowe, Cold Spring Harbor Laboratory, Cold Spring Harbor, NY) (17, 35). BOSC-23 cells were transiently transfected with the retroviral vector using lipofectamine (Invitrogen). Viral supernatants were collected 24 and 48 h after transfection and cleared by filtration. Two milliliters of filtered viral supernatant was added to *caspase-2*$^{+/+}$ and *caspase-2*$^{-/-}$ MEFs at 80% confluency and incubated for 24 h. Infected cell populations were selected by culture in hygromycin B.

In Vivo Tumor Growth and Histological Analysis. Suspension of pWZL-H E1A/Ras-transformed *caspase-2*$^{+/+}$ and *caspase-2*$^{-/-}$ MEFs (1×10^6 cells in 200 μL sterile PBS) were injected s.c. into both hind flanks of male 6- to 8-week-old *Balbc* athymic nude mice (supplied by the University of Adelaide Animal Facility, Adelaide, Australia), and tumors were allowed to develop for up to 20 days. Tumors were measured externally with a caliper, in 2 dimensions on indicated days. Tumor volumes were calculated from the equation $V = (L \times W^2) \times 0.5$, where L is length and W is width (36). Blood and tissue samples were collected from animals for histological examination. Tumors were collected in 10% buffered neutral formalin, paraffin processed, sectioned, and stained with hematoxylin and eosin.

Animal Studies. Eμ-*Myc*, *Bim*, and *caspase-2* knockout (KO) and athymic Balb-c mice were used in this study. All animals were housed and treated in accordance with protocols approved by the Institute of Medical and Veterinary Science (IMVS)/Central Northern Adelaide Health Services Animal Ethics Committee. Eμ-*Myc* transgenic, *caspase-2*$^{-/-}$, and *Bim*$^{-/-}$ mice were obtained from Jerry Adams, David Vaux, and Andreas Strasser (Walter and Eliza Hall Institute, Melbourne, Australia) (8, 18, 25). Eμ-*Myc* transgenic mice have been backcrossed onto the C57BL/6J background for more than 20 generations (21). *Bim*$^{-/-}$ and *caspase-2*$^{-/-}$ mice have been backcrossed to C57BL/6J mice for 12 and 8 generations, respectively (8, 25). All mice were rederived at the IMVS animal resource

facility. Eμ-*Myc* males were crossed with *caspase-2*$^{-/-}$ or *Bim*$^{+/-}$ females. Then, caspase-2$^{+/-}$/Eμ-*Myc* male offspring were crossed with *caspase-2*$^{-/-}$ females to generate *caspase-2*$^{-/-}$/Eμ-*Myc* mice. Similarly, *Bim*$^{+/-}$/Eμ-*Myc* male offspring were crossed with *Bim*$^{-/-}$ females to generate *Bim*$^{-/-}$/Eμ-*Myc* mice. The Eμ-*Myc* transgene and the KO alleles were detected by PCR. The *Myc* transgene was always bred through the male because differences in lymphoma onset have been observed between offspring from Eμ-*Myc* males versus offspring from Eμ-*Myc* females (20). Many Eμ-*Myc* females develop lymphoma while rearing their offspring and are therefore poor mothers (20).

Mice of each genotype were monitored daily for tumor development. Rate and incidence of lymphoma in cohorts of recipient mice were compared by log rank test and Kaplan-Meier analysis using the GraphPad Prism 4 software. Cause of death was attributed to Eμ-*Myc* lymphoma if a combination of the following features were noted: presence of enlarged spleen and/or lymph nodes, histologic evidence of invasive lymphoma, and/or lymphocyte count $>20 \times 10^6$/mL. Tumors, peripheral blood, and tissue samples were collected after euthanization of sick mice. Lymphoma cells from tumors were cultured in DMEM media with 10% FBS supplemented with 50 μM β-mercaptoethanol and 100 μM asparagine for further studies. All mice used for breeding were censored from the analysis at the time of mating to exclude any effect of breeding on tumor development. Pre-B or B-cell lymphomas were assessed by surface staining of Ig-M-positive or -negative cells by flow cytometry (21).

Analysis of *p21* Expression. Total RNA was isolated from MEF using TRIzol reagent (Invitrogen). cDNA was synthesized from 1 μg RNA using high-capacity cDNA reverse transcription kit (Applied Biosystems) and random primers. Real-time PCR was performed on a Rotor-Gene 3000 (Corbett Research) using RT^2 Real-Time SYBR Green/ROX PCR Master Mix (Superarray) as per the manufacturer's instructions. The following primer sets were used. *p21*: AGTGTGCCGTTGTCTCTTCG and ACACCAGAGTGCAAGACAGC; *β-actin*: GATCATTGCTCCTCCTGAGC and AGTCCGCCTAGAAGCACTTG. Reactions were performed in triplicate and the mRNA expression levels normalized against the internal control gene *β-actin* using the $\Delta\Delta C_T$ method.

Cell Death Analysis. *Caspase-2*$^{+/+}$ and *Caspase-2*$^{-/-}$ MEFs, or lymphoma cells derived from Eμ-*Myc*, *Caspase-2*$^{-/-}$ Eμ-*Myc*, and *Bim*$^{-/-}$ Eμ-*Myc* mice, were incubated with various drugs at indicated concentrations. Apoptosis was determined by Annexin V (Roche) and propidium iodide staining using flow cytometry (14). Where indicated, transformed and nontransformed *caspase-2*$^{+/+}$ and *caspase-2*$^{-/-}$ MEFs were irradiated (10 Gy) with or without 1 μM Gö6976 (Calbiochem) and incubated for 48 h before staining with Annexin V.

Caspase Assays. Caspase assays were carried out essentially as described (31, 37) using VDVAD-AMC (California Peptide Research) and DEVD-AMC (Enzyme System Products) as substrates. Fluorescence was analyzed on a FLUOstar Optima Luminescence Spectrometer (BMG Labtech; excitation 355 nm, emission 460 nm). Results from independent experiments were expressed as relative fluorescence units.

Caspase-2 Knockin. Caspase-2-GFP construct (2 μg) was transfected into nontransformed and transformed *caspase-2*$^{-/-}$ MEFs with lipofectamine (Invitrogen). After 48 h, cells were γ-irradiated (10 Gy) and apoptosis assessed at indicated times by Annexin V staining using flow cytometry. As overexpression of caspase-2 leads to apoptosis, dead cells (presumable expressing very high levels of caspase-2) were washed out before irradiating cells. Lysates from transfected cells were immunoblotted using a caspase-2 antibody (8) and a β-actin antibody (Sigma).

BrdU Incorporation. 1×10^5 MEFs or MEFs transformed with E1A/Ras were seeded on coverslips in 6-cm dishes and exposed to 10 Gy γ-radiation 16 h later. Following 24 h, cells were pulsed with 30 μM BrdU for 4 h. Cells were washed and fixed in cold 70% ethanol, hydrolyzed in 2M HCl in PBS, blocked in 1% BSA in PBS for 1 h, and incubated with anti-BrdU (BD Pharmingen) overnight at 4 °C. After washing, cells were incubated with mouse Alexa 488 antibody for 1 h and counterstained with Hoechst dye (Roche). Coverslips were mounted in antifade solution (1% propylgalate, 87% glycerol) and fluorescence images captured using an epifluorescence microscope (model BX51; Olympus) and a camera (U0CMAD3/CVM300; Olympus). Because of the loss of some cells resulting from apoptosis induced by γ-irradiation, the data in Fig. 5 provides an approximate percentage of cells in S phase.

Statistical Analysis. Statistical analyses were performed with Student's *t* test unless stated otherwise. Where appropriate, the data are expressed as mean $\pm$ SEM. The *P* values of <0.05 were considered significant.

ACKNOWLEDGMENTS. We thank Jerry Adams, David Vaux, Scott Lowe, Clare Scott, and Andreas Strasser for providing mice and reagents, staff at the Institute of Medical and Veterinary Science animal facility for help in maintaining the strains, and Thomas Sullivan for advice on statistical analysis of data. We thank members of our laboratory for helpful discussions. This work was supported by the National Health and Medical Research Council of Australia Grant 453482 and Fellowship 399300 (to S.K.).

1. Evan GI, Vousden KH (2001) Proliferation, cell cycle and apoptosis in cancer. *Nature* 411:342–348.
2. Danial NN, Korsmeyer SJ (2004) Cell death: Critical control points. *Cell* 116:205–219.
3. Kumar S (2007) Caspase function in programmed cell death. *Cell Death Differ* 14:32–43.
4. Kumar S, Kinoshita M, Noda M, Copeland NG, Jenkins NA (1994) Induction of apoptosis by the mouse Nedd2 gene, which encodes a protein similar to the product of the Caenorhabditis elegans cell death gene ced-3 and the mammalian IL-1 beta-converting enzyme. *Genes Dev* 8:1613–1626.
5. Kumar S, Tomooka Y, Noda M (1992) Identification of a set of genes with developmentally down-regulated expression in the mouse brain. *Biochem Biophys Res Commun* 185:1155–1161.
6. Wang L, Miura M, Bergeron L, Zhu H, Yuan J (1994) Ich-1, an Ice/ced-3-related gene, encodes both positive and negative regulators of programmed cell death. *Cell* 78:739–750.
7. Bergeron L, et al. (1998) Defects in regulation of apoptosis in caspase-2-deficient mice. *Genes Dev* 12:1304–1314.
8. O'Reilly LA, et al. (2002) Caspase-2 is not required for thymocyte or neuronal apoptosis even though cleavage of caspase-2 is dependent on both Apaf-1 and caspase-9. *Cell Death Differ* 9:832–841.
9. Kumar S, et al. (1995) Apoptosis regulatory gene NEDD2 maps to human chromosome segment 7q34–35, a region frequently affected in haematological neoplasms. *Hum Genet* 95:641–644.
10. Faderl S, et al. (1999) Caspase 2 and caspase 3 as predictors of complete remission and survival in adults with acute lymphoblastic leukemia. *Clin Cancer Res* 5:4041–4047.
11. Estrov Z, et al. (1998) Caspase 2 and caspase 3 protein levels as predictors of survival in acute myelogenous leukemia. *Blood* 92:3090–3097.
12. Holleman A, et al. (2005) Decreased PARP and procaspase-2 protein levels are associated with cellular drug resistance in childhood acute lymphoblastic leukemia. *Blood* 106:1817–1823.
13. Hofmann WK, et al. *(2001)* Altered apoptosis pathways in mantle cell lymphoma detected by oligonucleotide microarray. *Blood* 98:787–794.
14. Ho LH, Read SH, Dorstyn L, Lambrusco L, Kumar S (2008) Caspase-2 is required for cell death induced by cytoskeletal disruption. *Oncogene* 27:3393–3404.
15. Mendelsohn AR, Hamer JD, Wang ZB, Brent R (2002) Cyclin D3 activates Caspase 2, connecting cell proliferation with cell death. *Proc Natl Acad Sci USA* 99:6871–6876.
16. Sidi S, et al. (2008) Chk1 suppresses a caspase-2 apoptotic response to DNA damage that bypasses p53, Bcl-2, and caspase-3. *Cell* 133:864–877.
17. Serrano M, Lin AW, McCurrach ME, Beach D, Lowe SW (1997) Oncogenic ras provokes premature cell senescence associated with accumulation of p53 and p16INK4a. *Cell* 88:593–602.
18. el-Deiry WS, et al. (1993) WAF1, a potential mediator of p53 tumor suppression. *Cell* 75:817–825.
19. Adams JM, et al. (1985) The c-myc oncogene driven by immunoglobulin enhancers induces lymphoid malignancy in transgenic mice. *Nature* 318:533–538.
20. Harris AW, et al. (1988) The Eμ-myc transgenic mouse. A model for high-incidence spontaneous lymphoma and leukemia of early B cells. *J Exp Med* 167:353–371.
21. Egle A, Harris AW, Bouillet P, Cory S (2004) Bim is a suppressor of Myc-induced mouse B cell leukemia. *Proc Natl Acad Sci USA* 101:6164–6169.
22. Scott CL, et al. (2004) Apaf-1 and caspase-9 do not act as tumor suppressors in myc-induced lymphomagenesis or mouse embryo fibroblast transformation. *J Cell Biol* 164:89–96.
23. Baptiste-Okoh N, Barsotti AM, Prives C (2008) A role for caspase 2 and PIDD in the process of p53-mediated apoptosis. *Proc Natl Acad Sci USA* 105:1937–1942.
24. Krelin Y, et al. (2008) Caspase-8 deficiency facilitates cellular transformation in vitro. *Cell Death Differ* 15:1350–1355.
25. Bouillet P, et al. (2002) BH3-only Bcl-2 family member Bim is required for apoptosis of autoreactive thymocytes. *Nature* 415:922–926.
26. Bouillet P, Cory S, Zhang LC, Strasser A, Adams JM (2001) Degenerative disorders caused by Bcl-2 deficiency prevented by loss of its BH3-only antagonist Bim. *Dev Cell* 1:645–653.
27. Bouillet P, et al. (1999) Proapoptotic Bcl-2 relative Bim required for certain apoptotic responses, leukocyte homeostasis, and to preclude autoimmunity. *Science* 286:1735–1738.
28. Lassus P, Opitz-Araya X, Lazebnik Y (2002) Requirement for caspase-2 in stress-induced apoptosis before mitochondrial permeabilization. *Science* 297:1352–1354.
29. Kumar S, Vaux DL (2002) A cinderella caspase takes center stage. *Science* 297:1290–1291.
30. Paroni G, Henderson C, Schneider C, Brancolini C (2002) Caspase-2 can trigger cytochrome C release and apoptosis from the nucleus. *J Biol Chem* 277:15147–15161.
31. Baliga BC, Read SH, Kumar S (2004) The biochemical mechanism of caspase-2 activation. *Cell Death Differ* 11:1234–1241.
32. Colussi PA, Harvey NL, Kumar S (1998) Prodomain-dependent nuclear localization of the caspase-2 (Nedd2) precursor. A novel function for a caspase prodomain. *J Biol Chem* 273:24535–24542.
33. Baliga BC, et al. (2003) Role of prodomain in importin-mediated nuclear localization and activation of caspase-2. *J Biol Chem* 278:4899–4905.
34. Lowe SW, Ruley HE, Jacks T, Housman DE (1993) p53-dependent apoptosis modulates the cytotoxicity of anticancer agents. *Cell* 74:957–967.
35. Hemann MT, et al. (2004) Suppression of tumorigenesis by the p53 target PUMA. *Proc Natl Acad Sci USA* 101:9333–9338.
36. Vasseur S, et al. (2002) p8 is critical for tumour development induced by rasV12 mutated protein and E1A oncogene. *EMBO Rep* 3:165–170.
37. Dorstyn L, Kumar S (2008) A biochemical analysis of the activation of the Drosophila caspase DRONC. *Cell Death Differ* 15:461–470.